Demonstration of catalytic properties of de-inking sludge char as a carbon based sacrificial catalyst

Fivga, Antzela; Jahangiri, Hessam; Bashir, Muhammad; Majewski, Artur; Hornung, Andreas; Ouadi, Miloud

DOI:
10.1016/j.jaap.2020.104773

Journal of Analytical and Applied Pyrolysis 146 (2020) 104773

Contents lists available at ScienceDirect

Journal of Analytical and Applied Pyrolysis

journal homepage: www.elsevier.com/locate/jaap

Demonstration of catalytic properties of de-inking sludge char as a carbon based sacrificial catalyst

Antzela Fivga[a,*], Hessam Jahangiri[a], Muhammad Asif Bashir[a], Artur J. Majewski[a], Andreas Hornung[a,b,c], Miloud Ouadi[a]

[a] University of Birmingham, School of Chemical Engineering, Edgbaston, Birmingham, B15 2TT, United Kingdom
[b] Fraunhofer UMSICHT, Fraunhofer Institute for Environmental, Safety and Energy Technology, An der Maxhütte 1, 92237, Sulzbach-Rosenberg, Germany
[c] Friedrich-Alexander University Erlangen-Nuremberg, Schlossplatz 4, 91054, Erlangen, Germany

ARTICLE INFO

Keywords:
Bioenergy
Paper industry
De-inking sludge
Pyrolysis
Char
Catalyst

ABSTRACT

De-inking sludge (DIS) is generated as a waste stream from secondary fibre paper mills during the de-inking stage of the paper pulping process; in order to ensure end of waste to landfill an alternative valorisation route is required for this waste. At the same time, an inexpensive sacrificial catalyst is essential to achieve the techno-economic feasibility of biomass gasification and pyrolysis. The present work explores the potential of DIS char as a catalyst using a 2 kg/h Thermo-Catalytic Reforming (TCR®) system, which involves intermediate pyrolysis combined with a unique integrated catalytic reforming step. Wood was used for the TCR catalytic experiments with a DIS char to biomass ratio (wt.%) of 0.3:1 and 0.65:1. Results have shown that hydrogen relative volumes and syngas yields, are positively correlated with the increase in DIS char to wood ratio. Average hydrogen relative volumes of 28.30 vol.% and syngas yields of 47.64 wt.% were achieved. Organic liquid yields were significantly reduced in favour of higher syngas yields, implying the suitability of DIS char as a tar reduction catalyst in gasification or pyrolysis. The influence of TCR DIS char is less profound on the chemical distribution in the organic phase of bio-oil; a reduction on PAHs from 38.82 % to 26.70 % though was determined with the use of DIS char, according to the relative abundance peak areas from the GC–MS chromatograms. The oxygen content of bio-oil was significantly reduced due to cracking of higher molecular weight organics.

1. Introduction

Pyrolysis is a promising process for the generation of sustainable fuels and green chemicals from lignocellulose materials and waste. The process involves the thermal decomposition of organic matter under the absence of oxygen to produce bio-oil, syngas, and char. The physio-chemical properties of bio-oil, such as oxygen content [1] and viscosity [2], vary significantly from those of conventional fossil derived fuels, thus significant upgrading is required for its use into existing engines or co-processing with fossil fuels. Current upgrading methods include zeolite cracking [3] and catalytic hydro treatment [4] where both of them require the use of costly catalysts. An inexpensive, sustainable alternative is required.

Furthermore, pyrolysis can be applied as a solution to waste management while generating valuable energy vectors. The paper and pulp industry produces a significant amount of waste material (up to 4.3 million tonnes in Europe), in particular from secondary (recycled) fibre mills, which generate significant tonnages of de-inking sludge (DIS), that is sent to be landfilled [5]. CEPI has reported that the total paper production in Europe was around 91 million tonnes, in 2016 [6], highlighting the need for sustainable waste disposal methods. With increasing gate fees and the introduction of the waste directive that prohibits landfilled of organic wastes, it is becoming increasingly costly and challenging for paper mills to dispose of these waste streams. Pyrolysis can provide a solution to the dual issue of waste management and sustainable energy generation.

Even though limited work has been carried out on the pyrolysis of DIS [7–9] it was not possible to identify any work which has investigated systematically the catalytic effect of DIS char. Lou et al. used a static bench scale tubular furnace to conduct pyrolysis experiments at 800 °C with DIS [7]. The results have shown that 45.81 wt.% of char was produced and it was mainly composed of calcium carbonate. Further work from Ouadi et al. was conducted using a 20 kg/h intermediate pyrolysis reactor [8]. The reactor temperature was set at 450 °C and 15 kg/h feeding rate. Approximately, 75 wt.% of char was generated, which was mainly calcium based. Mendez et al. also studied the

* Corresponding author.
E-mail address: a.fivga@bham.ac.uk (A. Fivga).

https://doi.org/10.1016/j.jaap.2020.104773
Received 15 July 2019; Received in revised form 16 December 2019; Accepted 10 January 2020
Available online 13 January 2020

pyrolysis behaviour of DIS using SEM, FTIR, DRX, and TGA techniques [9]. It was also revealed that deinking sludges contain high $CaCO_3$ content with approximately 46.9 wt.%.

This paper focuses on demonstrating the catalytic properties of char derived from Thermo-Catalytic Reforming (TCR®) of DIS. The TCR technology combines intermediate pyrolysis and post catalytic reforming; intermediate pyrolysis stage takes place under moderate solid and vapour residence times (approximately 15 min) and reaction temperatures ranging from 400 to 550 °C generating high yields of condensable and non-condensable organic vapours, as well as, char; during reforming the catalytic cracking of vapours occurs at elevated temperatures (up to 700 °C) to promote further the formation of organic vapours, which when condensed, yield de-oxygenated bio-oil, as well as, synthesis gas [10]. As it was mentioned, previous work has shown that DIS char was mainly composed of calcium carbonate. Research has explored the importance of CaO as a catalyst in biomass gasification and pyrolysis [11–16]. It is well-known that compounds of alkali and alkaline earth metals (AAEMs) are active catalysts for bio-oil upgrading, as well as, for tar cracking in gasification [17]. Ca-based catalysts are also active for pyrolysis of naphtha related substances [18,19]. Early work has presented that DIS derived char has catalytic properties similar to that of dolomite or limestone [7–9]. The similar properties of DIS ash to those of dolomite could lead to the development of a promising tar cracking catalyst used in gasification. In addition to the AAEMs present in char, the amorphous carbon structure of char with active surface functional groups also contributes to its high catalytic activity [20]. Therefore, the proposed TCR technology simultaneously utilises deinking sludge and produces valuable catalytically active char, as well as, biofuels.

In the present work, DIS was processed in a 2 kg/h TCR reactor, generating char, with the aim of assessing its potential as a sacrificial catalyst. Wood was used as a reference feedstock for the TCR catalytic experiments. The amount of wood for each run was fixed while the DIS char to biomass ratio (wt.%) was increased (0.3:1.0) and (0.65:1.0) was used. Results are presented from the intermediate pyrolysis experiments themselves along with the full characterisation of the products formed from TCR of wood and the catalytic runs with different ratios of char.

2. Materials and methods

2.1. Raw materials and pre-treatment

DIS was acquired from DS Smith Kemsley Paper Mill in Sittingbourne, Kent. DS Smith Kemsley Paper Mill is a secondary fibre paper mill, which uses recycled paper to manufacture newsprint; DIS is a waste residue produced during the de-inking stage of this process. This solid waste residue consists of fillers, inks, pigments, short length fibres, dyes, and adhesives, which are derived from the initial recycled paper feedstock. Pine wood pellets were used as a reference feedstock for the TCR experiments.

The DIS feedstock as received contained an average moisture content of 50 wt.%. This was dried to a moisture content of approximately 15 wt.% using a Memmert UF750 oven at 80 °C for 8 h. The dry material was then pelletised using a DORN-TEC PTE 50 pelletiser to ensure blockage-free operation in the TCR. The pellets formed were approximately 6 mm diameter by 15 mm length.

The DIS/wood pellets for the catalytic runs were produced by mixing DIS char and pine wood at a DIS char to biomass ratio (wt.%) of 0.3:1 and 0.65:1. The same pelletisation method as the DIS feedstock was followed producing pellets of approximately 6 mm diameter by 15 mm length.

2.2. Thermogravimetric analysis (TGA)

The proximate analysis, as well as, the thermal degradation behaviour of the samples, were determined using a NETZSCH TG 209 Thermogravimetric Analyser (TGA) following the E1131-03 ASTM standard [21]. Each sample was ground and sieved. Each experiment was carried out in duplicates. Approximately 12 mg of each sample was used for the analysis. The sample was heated at 20 °C/min in a purge of nitrogen at a flow rate of 30 ml/min with a maximum temperature of 900 °C and each sample was held at the maximum temperature for 15 min. To determine the ash content, the same programme was used but under air atmosphere. The amount of moisture content, volatile matter, and ash content in each sample were determined by the TGA. The fixed carbon content was calculated by difference.

2.3. X-ray powder diffraction (XRD)

Phase identification was carried out, for the DIS char samples, as well as, wood char, by wide angle XRD using a Bruker D8 Advance diffractometer and Cu Kα radiation over a diffraction 2θ angle from 10° to 80° with a step size of 0.05°. The crystallite size was calculated using the Scherrer equation:

$$\text{dcrystallite size (nm)} = \frac{0.94\lambda}{B \times cos\theta} \quad (1)$$

where B equals to the full-width at half-maximum (FWHM) of the most intense peak in the spectrum; and λ is the wavelength.

2.4. Elemental analysis and calorific values

Elemental analysis and calorific values of the feedstock, bio-oil, and char, were carried out by a Carlo-Erba EA1108 analyser. Elemental compositions (C, H, N, S) were obtained. Then, the oxygen content was calculated by difference (100 % - Σ (CHNS + ash)). The analysis was performed on duplicates of each sample, and average values were taken.

2.5. Experimental apparatus

The TCR system was used to process DIS and perform the catalytic experiments. The system consisted of a feed hopper, an intermediate pyrolysis auger reactor followed by a fixed bed reforming reactor with impinger tube for gas extraction, condensation system, filtration, and gas totaliser/analyser. Fig. 1 shows a detailed schematic of the TCR system. Initially, the feedstock (pellets) was pyrolysed at 450 °C, with a heating rate of 1 °C/s, in the complete absence of oxygen. Nitrogen was used as a purge gas. The total reactor length was 1 m, with an average solid residence time of fewer than 20 min. The pyrolysed material was then conveyed into the post-stage reformer along with the pyrolysis vapours, where catalytic cracking of vapours occurs at 650 °C; reforming reactions occurred between char and pyrolysis vapours to form condensable organic vapours and synthesis gas. The TCR system was heated externally using ceramic band heaters. It should be noted that the pellets crumbled into powder before entering the post-stage reformer. The condensable organic vapours and synthesis gas exited the post reformer into the condensation system. The system consisted of a shell and tube condenser (cooling medium water-glycol mixture cooled to -5 °C) and an ice bath cooler, where vapours were condensed to form bio-oil. The bio-oil collected from the shell and tube condenser and the ice bath cooler was subjected for analysis. The remaining vapours (synthesis gas) were passed into a series of washing bottles, one filled with biodiesel, and the others filled with isopropanol and fiberglass wool for aerosol capture, and then subsequently directed to a gas analyser for detection. Biodiesel is an effective trap for non- polar heavy hydrocarbons and tars, while isopropanol is the standard solvent according to the ECN protocol/standard for sampling tars in syngas [22,23]. The gas analyser was fitted with an upstream carbon bag filter to protect against harmful contaminants and particulates. Lastly, the permanent gases were flared.

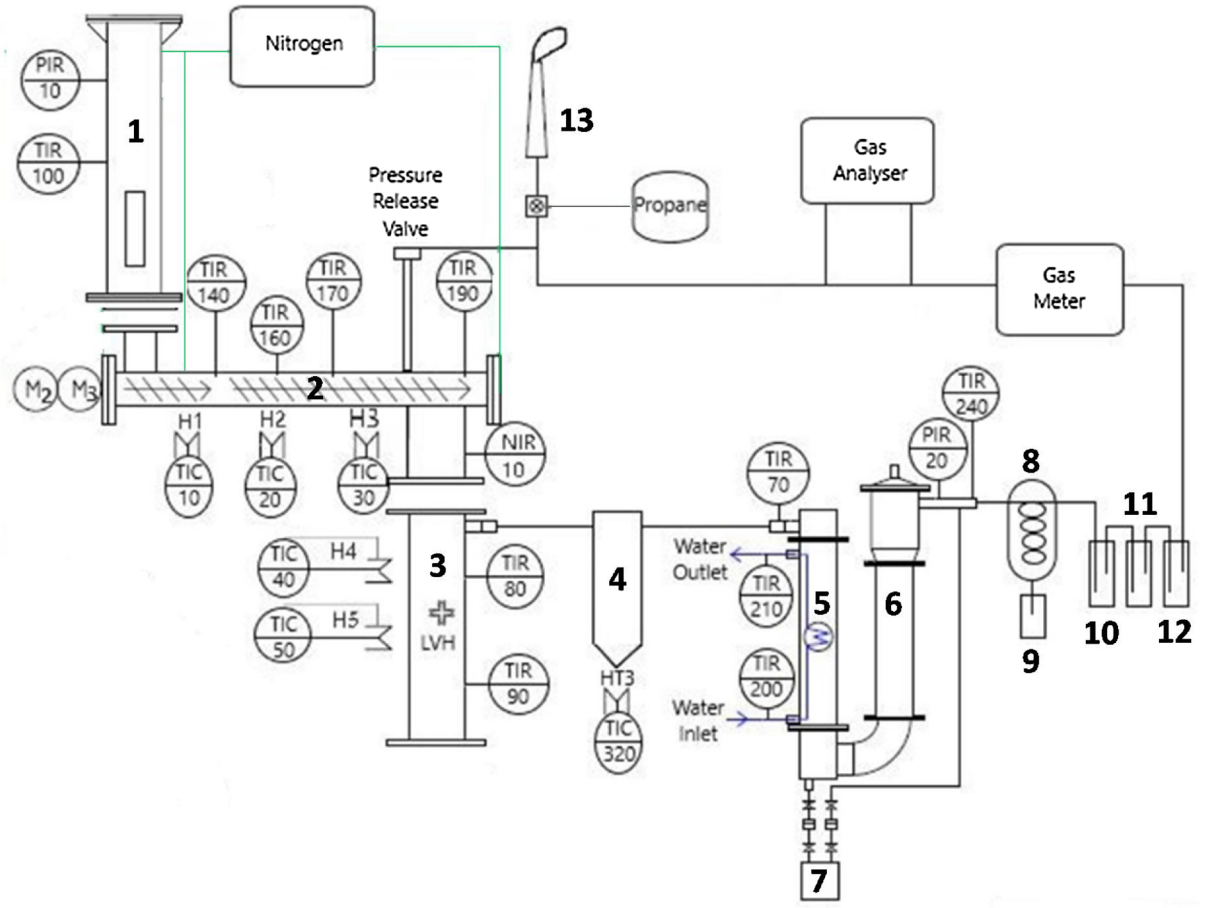

1. Feed hopper, 2. Auger reactor, 3. Post reformer, 4. Cyclone, 5. Shell and tube heat exchanger, 6. Scrubber, 7. Bio-oil collection vessel, 8. Ice bath, 9. Bio-diesel wash bottle, 10. Iso-propanol wash bottle, 11. Acetone wash bottle, 12. Wool bottle and 13. Flare.

Fig. 1. Process flow diagram (PFD) of the TCR (2 kg/h) plant.
1. Feed hopper, 2. Auger reactor, 3. Post reformer, 4. Cyclone, 5. Shell and tube heat exchanger, 6. Scrubber, 7. Bio-oil collection vessel, 8. Ice bath, 9. Bio-diesel wash bottle, 10. Iso-propanol wash bottle, 11. Acetone wash bottle, 12. Wool bottle and 13. Flare.

2.6. Bio-oil characterisation

2.6.1. Liquid GC–MS

GC–MS analysis was performed using an Agilent A7890 Gas Chromatograph coupled to a Waters Micromass Ltd GCT Premier Mass Spectrometer. A ZB5 Phenomenex versatile low polarity column (30 m × 0.25 mm × 0.25 µm) was used for the analysis of the organic fraction of bio-oil, while a ZBWAX plus (30 m × 0.25 mm × 0.25 µm) was used for the aqueous phase of bio-oil. The gas chromatograph used for compound separation had a split ratio of 1:10 using helium as the carrier gas at a constant flow rate of 1 ml/min. The initial oven temperature was 50 °C and ramped up to 300 °C with a heating rate of 2.5 °C/min. The mass spectrometer had an electron energy of 70 eV, trap current of 98 uA, and an emission current of 382.2 µA at a frequency of 0.9 scan/s within the $40-800\ m/z$ range. The compounds were identified by library searches (NIST libraries) and mass spectra evaluation and, were quantified in terms of relative abundance of peak area (% peak area to the total area). The organic samples were diluted in dichloromethane solution prior to analysis while the aqueous samples were injected as received.

2.6.2. Water content, density, and TAN

The water content of bio-oils was determined by Karl Fischer titration in accordance with ASTM D1744. A density meter was used to determine the density of bio-oils in accordance with ASTM method D4052. Total acid number (TAN) of bio-oil samples was determined by manual titration in accordance with ASTM D664.

2.7. Synthesis gas

For the online gas measurement, a calibrated gas detection system (GAS 3160 P Syngas Analyser and calorimeter) was used. The gas analyser was calibrated with calibration gases prior to commencing experiments. The measurement principle of the gas analyser is based on a non-dispersive infrared sensor (CO, CO_2, CH_4, C_nH_m), an electron capture detector (O_2), and a thermal conductivity detector (H_2).

3. Results and discussion

3.1. Feedstock composition and characteristics

Proximate, ultimate, and calorific values for wood and DIS are shown in Table 1. The values are reported on a dry basis by weight percent and are in agreement with typical findings in literature [8]. It can be observed from Table 1 that DIS had significantly lower heating values (9.8 MJ/kg) when compared with wood (23.1 MJ/kg). This is due to the high ash content of DIS. It has been reported elsewhere [8] that the composition of DIS ash is composed of mostly calcium and

Table 1
Proximate, ultimate, and higher heating values of wood and DIS.

	Wood	DIS
Moisture (as received) wt%	6.50	50.0
Moisture (dry basis) wt%	6.50	1.40
Proximate analysis wt.% (moisture free basis)		
Volatiles	84.94	57.04
Fixed carbon	13.85	0.78
Ash (at 900 °C)	1.21	42.18
Ash (at 575 °C)	1.21	64.00
HHV (MJ/kg) (dry basis)	24.30	10.20
LHV (MJ/kg) (dry basis)	23.10	9.80
Ultimate analysis wt.% (moisture free basis)		
Carbon	46.41	22.99
Hydrogen	6.14	2.60
Nitrogen	< 0.10	< 0.10
Sulphur	< 0.10	< 0.10
Oxygen (by difference)	46.04	10.21

aluminium based metal oxides.

Fig. 2 shows the differential thermogravimetric (DTG) profiles for the wood and DIS samples. The derivative weight of the samples is reported as the percentage weight loss per minute. It can be seen that the samples had different rate of maximum weight loss and peak temperature. The extent of the maximum degree of weight loss was more profound for the wood sample when compared with DIS. It should be noted that the extent of the maximum thermal decomposition rate is reflective of the cellulose, hemicellulose, and lignin content [24]. It can also be observed that the maximum rate of weight loss for wood occurs at approximate at 367 °C, while for DIS it occurs at 328 °C. The decomposition of cellulosic fibres and other de-inking minerals takes place at 328 °C for DIS. Furthermore, DIS had a second peak at 765 °C. This second peak was as a result of the thermal decomposition of $CaCO_3$ present within the ash and release of CO_2 [12]. The reason that DIS had a lower peak temperature (328 °C) than wood (367 °C) could be due the high calcium content that catalyses the thermal degradation process and subsequently lowers the main decomposition temperature. The shoulder at 367 °C wood peak may due to the cellulose–hemicellulose overlapping with lignin.

3.2. TCR experiments

The main aim of this work was to investigate the effect of pyrolysis char as a sacrificial inexpensive carbon based catalyst, and specifically DIS derived char, on pyrolysis products yield and composition. Pine wood was used as the reference feedstock. DIS char was produced from the pyrolysis of DIS in the TCR system using the same operating conditions (pyrolyser at 450 °C; post-reformer at 650 °C) as the pine wood and the catalytic runs to avoid further devolatilisation of the DIS char. The amount of catalyst (DIS char) mass used was calculated according to the catalyst to biomass ratio. The amount of wood for each run was fixed at 4 kg, while the catalyst to biomass ratio (wt.%) was 0.3:1 and 0.65:1.

Table 2
Mass balance of TCR non-catalytic and catalytic runs of wood and DIS char, expressed on biomass wt.%.

Feedstock	Pure wood	DIS char/wood 0.3:1	DIS char/wood 0.65:1
Char	**23.03**	**25.77**	**26.23**
Gases	**35.76**	**46.74**	**47.94**
Total liquids	41.21	27.50	25.83
Bio-oil (organics)	**20.95**	**7.94**	**6.31**
Aqueous	20.26	19.56	19.52

The TCR product yields, of raw wood and mixtures of wood with DIS char, have been calculated through Eq. 2 and results are presented in Table 2.

$$\Sigma \text{ Feedstock}_{\text{mass in}} = \Sigma \text{ (Gas + Char + Organics + Aqueous)}_{\text{mass out}} \quad (2)$$

Previous work reported on the TCR processing of raw wood has shown that char yields are typically within 20–23 wt.% [10] which is in agreement with the char yields (23 wt.%) produced in this work. In contrast, the organic (20.95 wt.%) and non-condensable gas (35.76 wt.%) yields produced vary significantly with previous TCR work but this could be due to the elevated temperature in the post-reformer used previously (750 °C) which accelerates the thermal cracking of pyrolysis vapours resulting in higher permanent gas yields and low bio-oil (organics) yields [25].

It can be observed from Table 2 that the increase in wood to char ratio affected the distribution of the resulting pyrolysis products. As the DIS derived char to wood ratio increased from 0.3:1 to 0.65:1, the yield of gases (syngas) and char increased from 46.74 wt.%, 25.77 wt.% to 47.94 wt.%, 26.23 wt.% respectively, while the organics yield decreased from 7.94 wt.% to 6.31 wt.%. Previous studies have shown that the use of biomass pyrolysis char as a catalyst can be effective in tar reduction due to its porous structure for higher absorbability and its inherent alkali and alkaline earth metallic species on the char surface [26,27]. In the case of DIS derived char, the high Ca content and other present alkaline earth metals could be responsible for the catalytic conversion of organics [12]. The increase of char and gaseous TCR

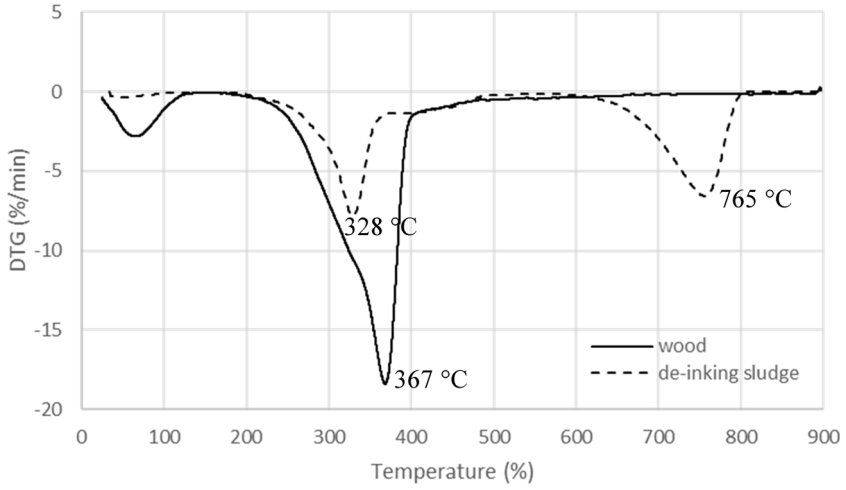

Fig. 2. Differential thermogravimetric (DTG) pyrolysis profiles for wood and DIS.

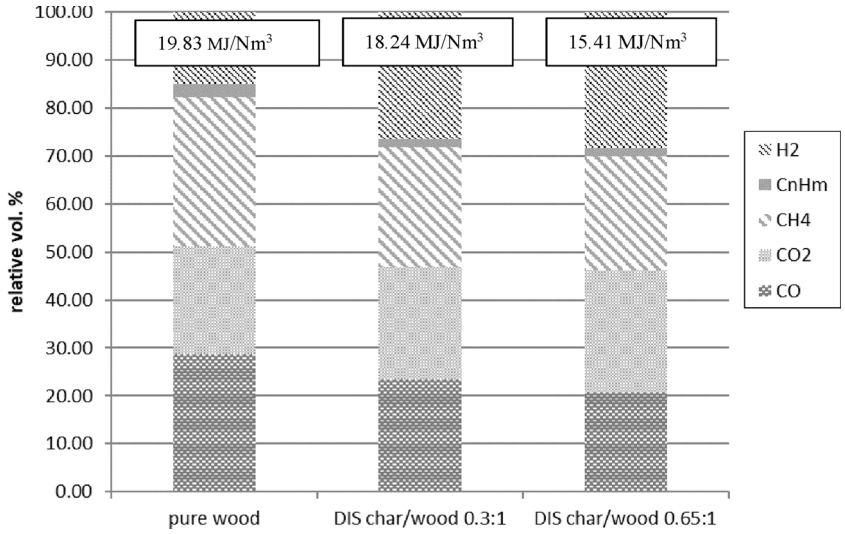

Fig. 3. Average relative normalised gas compositions (excluding nitrogen and non-identified compounds).

products is positively correlated with the increased of wood to DIS char ratio. This is in accordance with the results in literature where is shown that the inherent AAEMs in biomass promote organic or tar decomposition and polymerisation reactions resulting in an increase of char and gaseous yields [26,28,29].

3.3. Pyrolysis products

3.3.1. Non-condensable gas composition

The TCR non-condensable gases consist of CO, CO_2, CH_4, C_nH_m, and H_2, with a heating value between 15.41 and 19.83 MJ/Nm^3. The normalised gas compositions (expressed as vol.%) are depicted in Fig. 3.

The highest heating value can be observed for the syngas derived from the non-catalytic run with wood; this is attributed to the high methane concentration (31.29 vol.%) in syngas. The use of biochar as a catalyst enhances tar cracking resulting in the generation of coke due to poly-alkylation and condensation of aromatics in the vapour phase [30]. A hypothesis could be that the hydrogenation of the coke ($C + 2H_2 \leftrightarrow CH_4$), which was produced as a result of the tar cracking on the biochar, increased further methane volumes at the expense of hydrogen. Steam reforming reactions have also been enhanced utilising the moisture on the feedstock as a steam source resulting in the increase of methane yields.

The opposite trend can be observed for the syngas produced from the catalytic runs; hydrogen concentrations increased at the expense of methane. Average hydrogen relative volume of 28.30 vol.% was achieved for DIS char to wood ratio of 0.65 in comparison with the non-catalytic wood run which had achieved values of 15.00 vol.%. Studies have shown that the catalytic activity of pyrolysis derived char is accredited to the char matrix (surface area, amorphous structure, etc.) and the presence of inherent AAEMs [31]. An explanation of the increasing volumes of hydrogen, when compared to raw wood, could be higher concentrations of calcium and aluminium based metal oxides present in the DIS. Hu et al. have investigated the catalytic effect of inherent AAEMs on yield and property of rice husk pyrolysis products by using water and HCl washing method to remove the AAEMs from the original feedstock [26]. It was shown that AAEMs promoted the main hydrogen production reactions such as water–gas shift and hydrocarbon reforming reactions. Zhang et al. have studied the pyrolysis behaviour of biomass with various Ca-based additives [12]. Hydrogen concentration was increased up to 42 vol.% with the addition of CaO which further confirms that the high CaO concentration in DIS derived char has promoted hydrogen generation. Further previous studies have reported that CaO is responsible for tar reduction/elimination and hydrogen production [32,33].

It can also be noticed from Fig. 3 that the relative concentration of CO is higher than CO_2 in the case of raw wood while the opposite trend can be observed for the catalytic runs. According to Tröger et al., the CO to CO_2 ratio is relative to changes in pyrolysis product yields [34]. Specifically, an increase in CO_2 can indicate a decrease in bio-oil yields and an increase in char and syngas yields [29]; this is in agreement with the product yields presented in Table 2. Furthermore, the presence of CaO can convert the acids in bio-oil to hydrocarbons and CO_2 by decarboxylation reactions but this is discussed in more detail in the bio-oil section below [35].

Another explanation could be that initially at 450 °C in the pyrolyser, CO_2 was captured by CaO because of carbonation reactions forming $CaCO_3$ (Eq. 3) and thus promoting water shift reactions and hydrogen increase (Eq. 4) which is consistent with the literature [26,36]. At the reformer temperatures (650 °C), $CaCO_3$ started decomposing which resulted to let out some of the CO_2. The water-gas shift reaction would be expected to reduce CO concentration which is in agreement with Fig. 3.

$$CaO + CO_2 \rightarrow CaCO_3 \quad (3)$$

$$CO + H_2O \rightarrow CO_2 + H_2 \quad (4)$$

It should be noted that the composition of syngas and pyrolysis product yields is a complex combination of the thermal decomposition and cracking products of each biomass component. Moreover, inter-reactions between these primary pyrolysis products occur resulting in the generation of secondary products. To add to this complexity, the catalytic activity of pyrolysis derived char matrix and the presence of inherent AAEMs also play a significant role since reactions such as Boudouard and decarboxylation can be favoured [17].

3.3.2. Bio-oil

The elemental composition and heating values of the bio-oils (organic phase) are presented in Table 3. Compared to the carbon (70.75 wt.%) and oxygen (20.53 wt.%) contents of the wood bio-oil, the carbon level increased to 75.24 and 77.30 wt.%, while the oxygen level decreased to 15.91 and 14.14 wt.%, with the increase of char to biomass ratio. The addition of DIS derived char also resulted in the increase of HHV and LHV of bio-oils. Table 3 also presented the physical features of the bio-oils. The total acid number (TAN), which indicates the fuel corrosivity to engine components, was found to increase with the use of DIS char as a catalyst, ranging from 8.5 mg KOH/g (wood) to 27.6 mg KOH/g (char/biomass 0.3:1). Even though the use of DIS char

Table 3
Ultimate analysis and heating values of DIS and wood derived bio-oil (organics), as received.

	Pure wood	char/wood 0.3:1	char/wood 0.65:1
Carbon	70.75	75.24	77.30
Hydrogen	7.69	7.78	7.38
Nitrogen	0.62	0.69	0.37
Sulphur	0.43	0.40	0.81
Oxygen (by difference)	20.53	15.91	14.14
HHV (MJ/kg)	35.36	37.05	37.23
LHV (MJ/kg)	33.71	35.38	35.64
Density (g/cm^3)	1.055	1.065	1.041
Acid number (mg KOH/g)	8.5	27.6	13.7
Water content (% w/w)	3.8	6.4	5.3

as a catalyst yield to higher TAN, values were significantly lower than that of typical biomass pyrolysis oils [1].

The Van Krevelen diagram in Fig. 4, illustrates that as the char to biomass ratio increased the molar ratio of H/C and O/C in produced oil decreased (producing a more stable oil). The O/C and H/C ratios of the bio-oil from pine wood biomass were 0.22 and 1.30, respectively. The increase in char to biomass ratio from 0.3:1 to 0.65:1 resulted in a molar ratio of O/C and H/C from 0.16 to 0.14 and 1.24 to 1.15, respectively. Ingram et al. conducted fast pyrolysis experiments in an auger reactor with pine wood where the reported values of O/C (0.56) and H/C (1.72) were higher than for the obtained in this work TCR bio-oils [37]. It is depicted in Fig. 4 that the catalytic bio-oil produced in this work is even lower than bio-oils after HDO treatment [38,39], and significantly lower that of typical fast pyrolysis bio-oils [40]. The low molar ratio of O/C and H/C, which has resulted from the use of DIS char as a catalyst, indicates an improvement on bio-oil stability and performance characteristics.

Fig. 5 shows the GC–MS detectable compounds in the organic fraction of bio-oil produced from the non-catalytic and catalytic TCR runs of wood. Previous work on pyrolysis of pine wood has shown that the produced bio-oil is typically a complex mixture of various oxygenated compounds including acids, aldehydes, alcohols, ketones, phenols, furans, and mono-, di-, and higher saccharides [37,41,42]. Fig. 5 and Table 4 show that the organic fraction of non-catalytic wood derived bio-oil consists mainly of mono and polycyclic aromatic hydrocarbons, their isomers, such as, indene, fluorene, pyrene etc., with few compounds of phenols (see peaks 7, 11, 12, 14, 16, 18), furans (see peaks 19, 20, 25, 38), and an acid (see peak 8). The explanation for the elimination of the majority of the oxygenated compounds typically found in wood derived bio-oil was due to the catalytic effect of wood derived char, which was formed in the lower zone of the reformer during the non-catalytic wood run. It can be assumed that the addition of pyrolysis char, enhanced depolymerisation and aromatisation reactions of higher reactivity oxygen aromatic compounds, resulting in the formation of polycyclic aromatic hydrocarbons (PAHs), which explains the lower oxygen content of the oil presented in Table 3 when compared with typical fast pyrolysis wood bio-oils.

Similar findings can be seen for the catalytic derived bio-oil indicating that the CaO in de-inking char showed little effect on the composition of bio-oil when compared with the char matrix itself. 4-methyl-phenol was detected to be the most abundant compound in the raw wood derived bio-oil (7.94 %) and the catalytic derived bio-oil (8.14–8.75%), followed by naphthalene (7.61 and 5.86–7.23%, respectively). Fig. 6 illustrates the relative content of compounds found in the organic and aqueous phase of the bio-oil. It can be seen that the relative content of phenols in organics, such as phenol and 4-methyl-phenol, increased with higher char to wood ratios, in comparison with the pure wood run, reaching values of 25.62 % and 26.94 %, respectively. This explains the increase of TAN in the bio-oil samples shown in Table 3. Similar findings have been reported by Guo et al. when using pyrolysis char and metal impregnated (Fe, Cu and K) char as a catalyst in a dual-stage reactor [29]. The opposite trend can be observed for the aqueous phase of the bio-oil, where phenolics decreased with the increase of char to wood ratio, from 78.32%–53.95 %.

High relative contents of mono- and poly-cyclic aromatic hydrocarbons were detected with values of 60.50 %, 42.30 %, and 47.79 % for pure wood, char/wood ratio of 3:1, and char/wood ratio of 6.5:1, respectively. It should be noted that the relative content of PAHs in the organic phase is reduced from 38.82 % to 26.70 %, with the addition of char. A reduction of PAHs in bio-oil is desirable since there are well known health and environment concerns with their use [43].

The suggested catalytic pathway is shown in Fig. 7. Aromatics formation from hemicellulose and cellulose derived anhydrosugars, supported by literature, involves acid catalysed dehydration to furans that are promoted on the char surface [44]. Furans undergo either Diels-Alder condensation to form benzofuran (C_8H_6O) and water or decarbonylation to form allene (C_3H) and CO_2. Decarbonylation of benzofuran can also take place to form benzene and CO or CO_2. However, produced allene can undergo either alkylation with other aromatics to form heavier aromatics and ethylene or oligomerisation to form a series of olefins [45]. The suggested catalytic pathway to aromatics formation from lignin involves the decomposition of lignin to guaiacols, followed

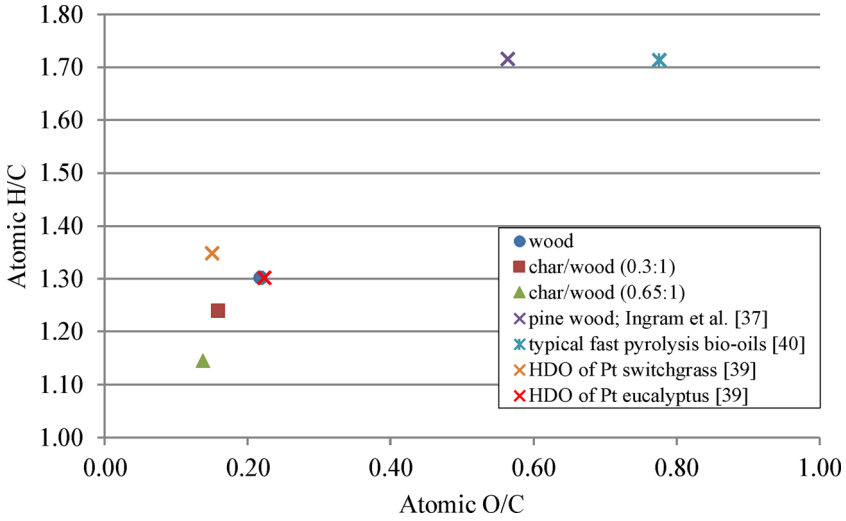

Fig. 4. Van Krevelen diagram of bio-oil from non-catalytic and catalytic wood, as well as, typical values of bio-oil from literature.

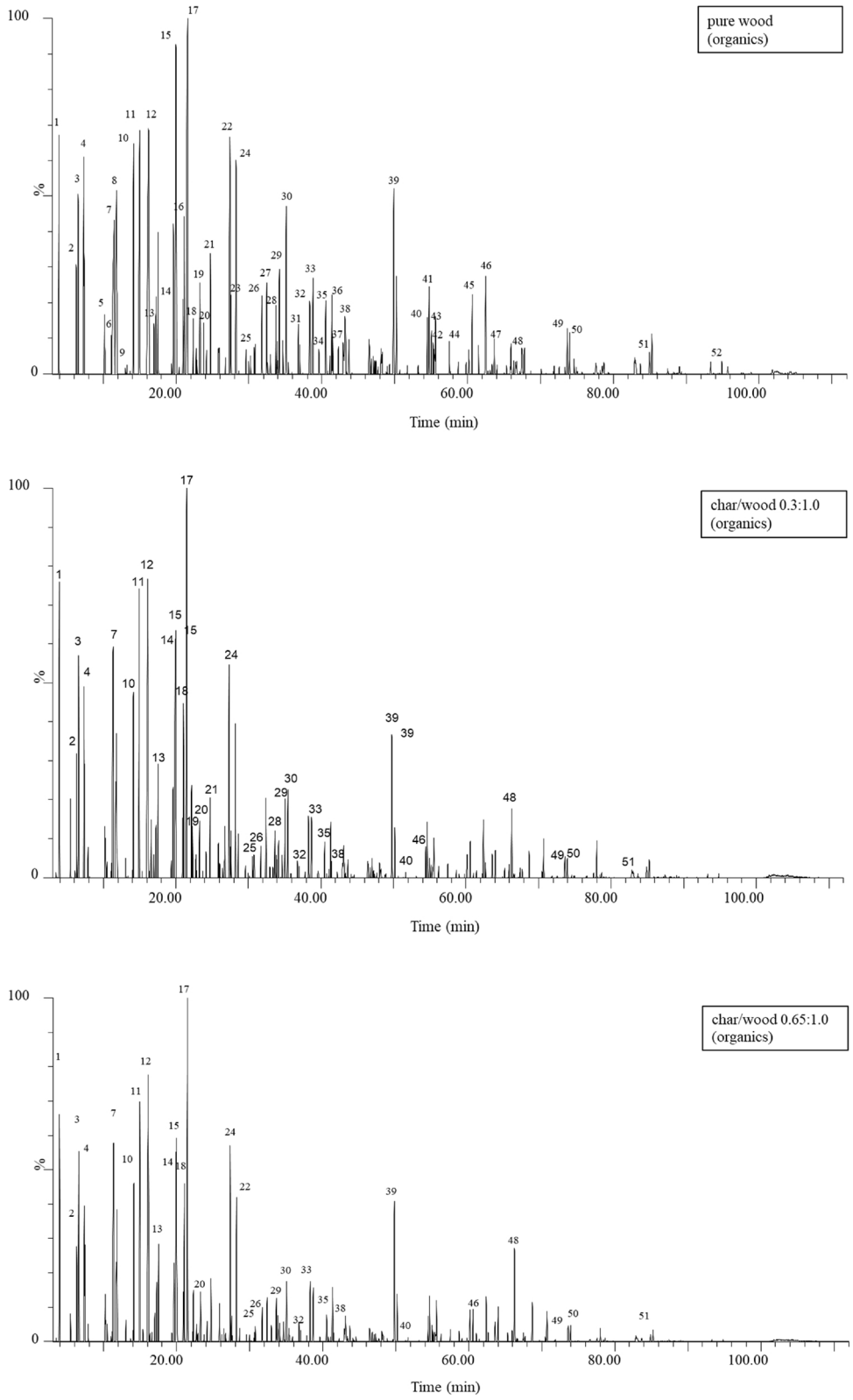

Fig. 5. Chromatogram obtained by GC–MS and chemical identification, organic fraction of non-catalytic and catalytic wood derived bio-oils. See Table 4 for key.

by the cracking of guaiacols to phenols by cleavage of the O—CH_3 bond [46]. Phenols can undergo further aromatic formation by cleavage of —OH. The carboxylic functional groups on the char surface are responsible for bio-oil upgrading.

Fig. 8 shows the chromatograms obtained from the GC–MS analysis of the aqueous fraction of bio-oil, respectively. In contrast to the organic fraction, the aqueous fraction contains oxygenated compounds including phenols, carboxylic acids, ketones, aldehydes, furans, and sugars. The common peaks of the chromatogram with the wood derived bio-oil are identified in Table 5. It can be noticed that acids are reduced with the addition of DIS char. Literature suggests that the de-acidification of CaO during pyrolysis could take place through the cracking,

Table 4
Identification of chemicals from the organic fraction of non-catalytic and catalytic wood derived bio-oils.

Peak Number	Retention Time	Chemical Name	Chemical Formula	Peak area (%)		
				Pure wood	char/wood (0.3/1)	char/wood (0.65/1)
1	3.94	Toluene	C_7H_8	2.07	2.76	2.88
2	6.29	Ethylbenzene	C_8H_{10}	1.07	1.19	1.18
3	6.56	Benzene, 1,3-dimethyl-	C_8H_{10}	1.67	2.32	2.46
4	7.31	Styrene	C_8H_8	2.97	2.93	2.82
5	10.99	Benzene, 1,2,3-trimethyl-	C_9H_{12}	4.11	ND	ND
6	11.11	Benzene, 1-ethenyl-2-methyl-	C_9H_{10}	0.72	ND	ND
7	11.53	Phenol	C_6H_6O	3.42	4.31	4.76
8	11.84	1,2-Benzenedicarboxylic acid, 4-methyl-	$C_9H_8O_4$	4.84	ND	ND
9	13.66	Indane	C_9H_{10}	0.37	ND	ND
10	14.18	Benzene, 1-propynyl-	C_9H_8	2.86	2.72	2.95
11	15.03	Phenol, 2-methyl-	C_7H_8O	4.08	4.63	4.69
12	16.21	Phenol, 4-methyl-	C_7H_8O	7.94	8.14	8.75
13	17.26	2-Propenal, 3-phenyl-	C_9H_8O	1.65	1.56	0.89
14	17.53	Phenol, 2,3-dimethyl-	$C_8H_{10}O$	1.79	1.67	1.90
15	19.66	Naphthalene, 1,2-dihydro-	$C_{10}H_{10}$	2.28	1.74	1.78
16	21.15	Phenol, 3-ethyl-	$C_8H_{10}O$	2.27	ND	ND
17	21.61	Naphthalene	$C_{10}H_8$	7.61	5.86	7.23
18	22.35	Phenol, 3,4-dimethyl-	$C_8H_{10}O$	1.03	6.87	6.96
19	23.3	Benzofuran, 2,3-dihydro-	C_8H_8O	1.58	1.36	1.38
20	23.78	Benzofuran, 2,3-dihydro-	C_8H_8O	0.96	1.36	1.38
21	24.73	Benzene, 1-methoxy-4-(4-methyl-4-pentenyl)-	$C_{13}H_{18}O$	1.56	1.02	
22	27.4	Naphthalene, 1-methyl-	$C_{11}H_{10}$	4.30	ND	2.98
23	27.55	Benzaldehyde, 4-ethyl-	$C_9H_{10}O$	0.85	ND	ND
24	28.23	Naphthalene, 2-methyl-	$C_{11}H_{10}$	3.33	3.20	3.77
25	29.6	Benzofuran, 7-methyl-	C_9H_8O	0.69	0.77	0.76
26	31.77	Biphenyl	$C_{12}H_{10}$	1.14	0.69	0.87
27	32.43	Naphthalene, 1-ethyl-	$C_{12}H_{12}$	1.84	0.02	ND
28	33.7	Naphthalene, 1,2-dimethyl-	$C_{12}H_{12}$	0.97	0.82	ND
29	34.18	Acenaphthene	$C_{12}H_{10}$	1.33	0.91	0.74
30	35.12	Acenaphthylene	$C_{12}H_8$	2.49	1.52	1.58
31	36.77	Acenaphthene	$C_{12}H_{10}$	0.86	0.91	0.74
32	36.98	1,1′-Biphenyl, 4-methyl-	$C_{13}H_{12}$	0.69	0.52	0.52
33	38.77	1-Naphthalenol	$C_{10}H_8O$	2.24	1.59	1.66
34	39.58	1,1′-Biphenyl, 4-methyl-	$C_{13}H_{12}$	0.90	0.52	0.52
35	40.53	Fluorene	$C_{13}H_{10}$	1.31	0.89	0.89
36	41.38	Fluorene	$C_{13}H_{10}$	2.03	0.89	0.89
37	42.27	Fluorene	$C_{13}H_{10}$	0.90	0.89	0.89
38	43.17	Dibenzofuran, 4-methyl-	$C_{13}H_{10}O$	1.76	1.03	0.80
39	49.87	Phenanthrene	$C_{14}H_{10}$	2.83	2.07	2.58
40	54.48	Anthracene, 2-methyl-	$C_{15}H_{12}$	0.67	0.54	0.57
41	54.7	Anthracene, 9-methyl-	$C_{15}H_{12}$	1.14	0.82	0.89
42	55.03	Anthracene, 2-methyl-	$C_{15}H_{12}$	0.64	0.54	0.57
43	55.25	4H-Cyclopenta[def]phenanthrene	$C_{15}H_{10}$	0.47	0.30	ND
44	57.5	Naphthalene, 2-phenyl-	$C_{16}H_{12}$	0.64	0.45	0.39
45	60.64	Fluoranthene	$C_{16}H_{10}$	1.20	0.67	0.98
46	62.47	Fluoranthene	$C_{16}H_{10}$	1.45	0.67	0.98
47	63.673	2-Phenanthrenol	$C_{14}H_{10}O$	0.82		
48	66.29	Phenanthrene, 1-methyl-7-(1-methylethyl)-	$C_{18}H_{18}$	0.31	0.91	1.58
49	73.68	Benz[a]anthracene	$C_{18}H_{12}$	0.52	0.39	0.32
50	74	Triphenylene	$C_{18}H_{12}$	0.56	0.42	0.34
51	84.93	Perylene	$C_{20}H_{12}$	0.37	0.21	0.26

neutralisation, and thermal cracking reaction pathways shown below [47,48]:

$$CaO + 2RCOOH \rightarrow (RCOO)_2 Ca + H_2O \quad (5)$$

$$(RCOO)_2 Ca \rightarrow CaCO_3 + RCOR \quad (6)$$

$$RCOOH \rightarrow CO_2 + RH \quad (7)$$

The carboxyl compounds in bio-oil can react with CaO resulting in the production of calcium carboxylate, which can decompose into $CaCO_3$ and ketones (Eqs. 5 and 6). Since the presence of ketones is not detectable in the DIS derived bio-oil, it can be assumed that thermal cracking has occurred simultaneously favouring the formation of CO_2 and hydrocarbons (Eq. 7).

An important consideration to make is the application of aqueous by-products from the process especially since the aqueous phase accounts for 20 % by mass of the overall products. Promising research has shown that the aqueous phase of bio-oil, also known as wood vinegar, has applications, such as crop pest control and soil microbial improvement [49,50].

3.3.3. Char characterisation

Tables 6 and 7 present the DIS and wood char composition and the metals retained within the char after the TCR experiments, respectively. The DIS char (16.85 wt.%) is much less carbonaceous than the wood char (90.18 wt.%). This is attributed due the high ash content of DIS char of 82.10 wt.%. Ca is the major constituent in the ash derived from both the DIS and wood char. The Ca level in DIS char (14.5 %) is significant higher than wood (3.58 %). This is due the mechanical agitation step at secondary fibre paper mills required to remove the fillers, inks, pigments, fibres and adhesives from the initial paper feedstock [8].

The DIS char samples were analysed by XRD technique to confirm

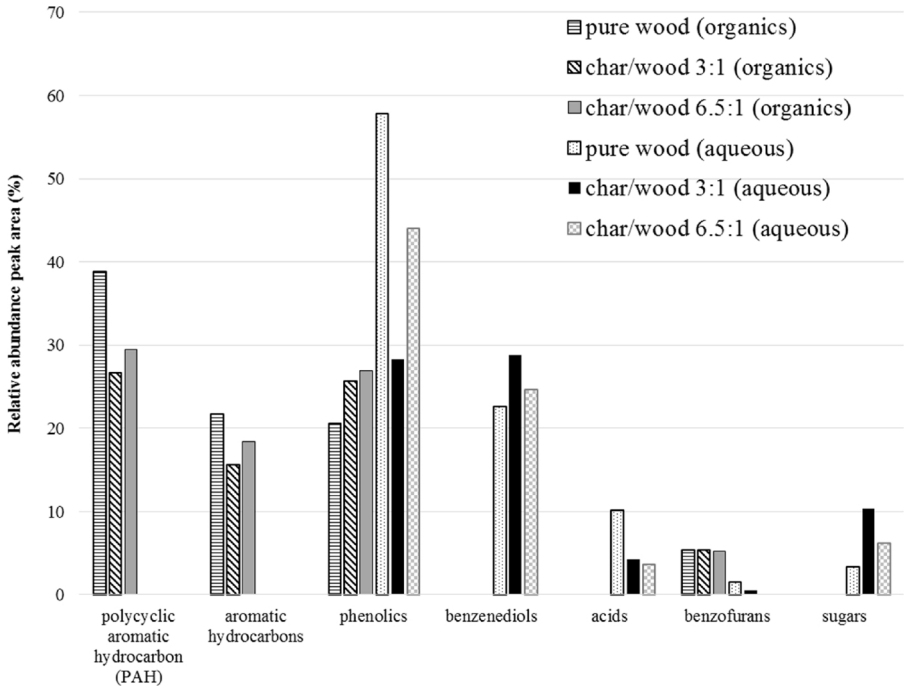

Fig. 6. Relative content of compounds detectable by GC–MS in the organic and aqueous fraction of bio-oil produced from pyrolysis of non-catalytic and catalytic wood.

the presence of Ca and their crystallinity. The XRD diffraction pattern of the DIS samples, as well as, the wood char sample, is shown in Fig. 9. Results showed that the main crystalline component for the DIS char samples is calcite with the most dominant peak at 29°. This corresponded with results for de-inking sludge from literature [51]. The crystallite size of the DIS char samples has not been significant affected after the catalytic runs, ranging from 45.26 nm for the fresh DIS char sample to 41.22 nm and 38.94 nm for the 0.3:1 and 0.65:1 ratios, respectively. The crystallite size was determined by Scherrer analysis based on the characteristic diffraction peaks of the DIS char samples at $2\theta = 29°$. Even though the crystal structure did not change, a decrease can be observed on the characteristic peak intensities after the use of DIS char as a catalyst. This may be due to the secondary polymerisation of pyrolysis intermediates (tar cracking), resulting in the production of coke and the covering of the diffraction peaks [47]. Regarding the wood char sample, the XRD diffraction pattern shows a broad characteristic peak around $2\theta = 22.5°$ and 44.3°, representing the crystal structure of amorphous silica and carbon, respectively [29,52].

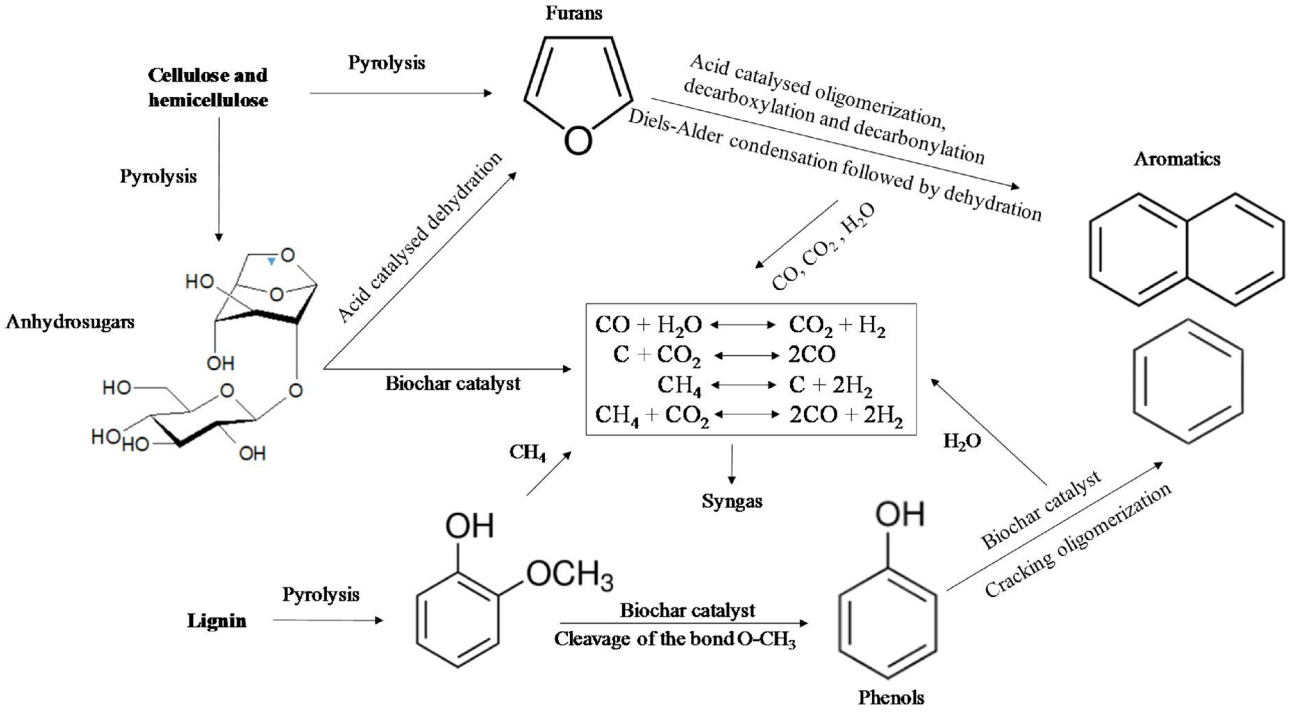

Fig. 7. Simplified scheme of reaction mechanisms for bio-oil species and syngas production using char (biochar) as a catalyst [45].

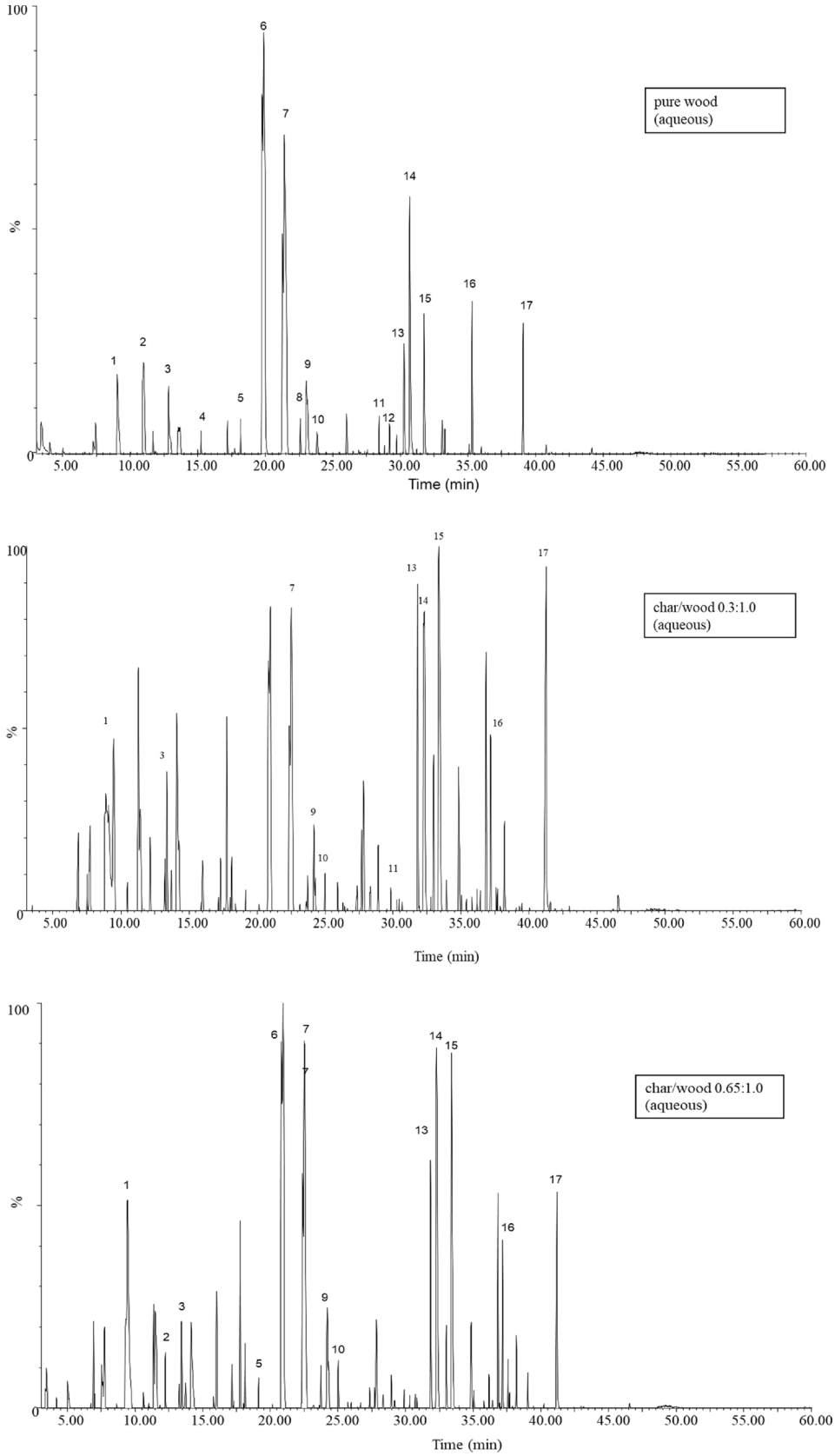

Fig. 8. Chromatogram obtained by GC–MS and chemical identification, aqueous fraction of non-catalytic and catalytic wood derived bio-oils. See Table 5 for key.

Table 5
Identification of chemicals from the aqueous fraction of non-catalytic and catalytic wood derived bio-oils.

Peak Number	Retention Time	Chemical Name	Chemical Formula	Peak area (%)		
				Pure wood	char/wood (0.3/1)	char/wood (0.65/1)
1	9.46	3-Furaldehyde	$C_5H_4O_2$	4.62	7.44	9.63
2	11.53	Propanoic acid	$C_3H_6O_2$	5.88	ND	1.79
3	13.48	Butanoic acid	$C_4H_8O_2$	3.61	3.11	1.84
4	16.03	Pentanoic acid	$C_5H_{10}O_2$	0.59	ND	ND
5	19.09	Phenol, 3,4-dimethyl-	$C_8H_{10}O$	0.93	ND	0.87
6	20.91	Phenol	C_6H_6O	21.29	ND	8.53
7	22.51	Phenol, 4-methyl-	C_7H_8O	21.32	9.25	11.96
8	23.77	Phenol, 2-ethyl-	$C_8H_{10}O$	1.06	2.42	3.06
9	24.23	Phenol, 3,4-dimethyl-	$C_8H_{10}O$	4.40	1.04	1.15
10	25.07	Phenol, 4-ethyl-	$C_8H_{10}O$	1.07	ND	ND
11	29.92	Benzofuran, 2-methyl-	C_9H_8O	0.83	0.52	ND
12	30.72	Benzofuran, 2-methyl-	C_9H_8O	0.71	ND	ND
13	31.86	1,2-Benzenediol, 3-methyl-	$C_7H_8O_2$	3.63	5.26	3.97
14	32.31	1,2-Benzenediol/Catechol	$C_6H_6O_2$	9.89	9.95	8.50
15	33.43	1,2-Benzenediol, 3-methyl-	$C_7H_8O_2$	5.13	10.91	8.57
16	37.18	Hydroquinone	$C_6H_6O_2$	3.97	2.68	2.36
17	41.18	1,6-Anhydro-á-D-glucopyranose (levoglucosan)	$C_6H_{10}O_5$	3.35	7.66	3.76

Table 6
Ultimate analysis and heating values of DIS and wood derived char, as received.

	Wood char	DIS char
Carbon	90.18	16.85
Hydrogen	1.57	0.62
Nitrogen	0.32	0.10
Sulphur	0.10	0.10
Oxygen (by difference)	3.63	0.24
Ash	4.20	82.10
HHV (MJ/kg)	33.20	6.67
LHV (MJ/kg)	32.86	6.54

Table 7
ICP analysis of DIS and wood derived char.

Elements	Wood char	DIS char	Units
Al	0.15	1.12	%
Ca	3.58	14.5	%
Fe	0.08	0.09	%
K	0.13	0.06	%
Mg	0.08	0.28	%
Mn	129	82	ppm
Na	46	293	ppm
P	118	220	ppm
Si	0.46	1.30	%
Sr	60	370	ppm
Ti	73	385	ppm

4. Conclusions

The proposed TCR technology simultaneously utilises DIS and produces valuable catalytically active char, as well as, biofuels. The experimental results from this work have demonstrated the potential of DIS char as an inexpensive carbon based sacrificial catalyst for biomass pyrolysis. The following conclusions have been drawn:

- The DTG analysis revealed that addition of DIS reduced the temperature needed for thermal decompositions of wood from 367 to 328 °C, which could be due to the high calcium content that catalyses the thermal degradation process. The utilisation of DIS char as a catalyst could result in a more energy efficient process since it lowers the main process decomposition temperature.
- The use of the TCR DIS char as a catalyst has shown potential for tar elimination in gasification. As the DIS char to wood ratio increased, organics yield decreased from 20.95 wt.% (non-catalytic wood) to 6.31 wt.% (0.65:1).
- Hydrogen relative volumes and syngas yields are positively correlated with the increase of DIS char to wood ratio. Average hydrogen relative volumes of 28.30 vol.% and syngas yields of 47.64 wt.% were achieved. The decarbonisation strategies in EU requires new uses of hydrogen to achieve the targets of 2050. The significant increase of hydrogen from the use of DIS char as a catalyst can provide the amounts of 'green' hydrogen required for EU's decarbonisation scenarios.
- Even though the use of DIS char as a catalyst yield higher total acid numbers, values were significantly lower in comparison with typical biomass fast pyrolysis oil.
- The catalytic effect of DIS char was more profound on the deoxygenation of bio-oil; the molar ratio of H/C and O/C decreased from 0.22 to 0.14 and 1.3 to 1.15, respectively. It seems that DIS char cracked and reformed the heavier molecular weight organic compounds resulting in the deoxygenation of the bio-oil (producing a more stable bio oil). This further reduces downstream processing costs for upgrading bio-oil to 'drop in' fuels. HHV increased for the catalytic bio-oil from 35.36 MJ/kg (pure wood) to 37.23 MJ/kg (DID char/wood; 0.65:1).
- The influence of TCR DIS char is less profound on the chemical distribution in the organic phase of bio-oil; a reduction on PAHs from 38.82 % to 26.70 % was determined by the increase in char to biomass ratio, according to the relative abundance peak areas from the GC–MS chromatograms.

Declaration of Competing Interest

The authors declare that they have no known competing financial interests or personal relationships that could have appeared to influence the work reported in this paper.

CRediT authorship contribution statement

Antzela Fivga: Conceptualization, Methodology, Data curation, Writing - original draft, Visualization, Writing - review & editing. **Hessam Jahangiri:** Methodology, Data curation, Writing - review & editing. **Muhammad Asif Bashir:** Methodology, Data curation. **Artur J. Majewski:** Funding acquisition. **Andreas Hornung:** Funding acquisition. **Miloud Ouadi:** Conceptualization, Funding acquisition.

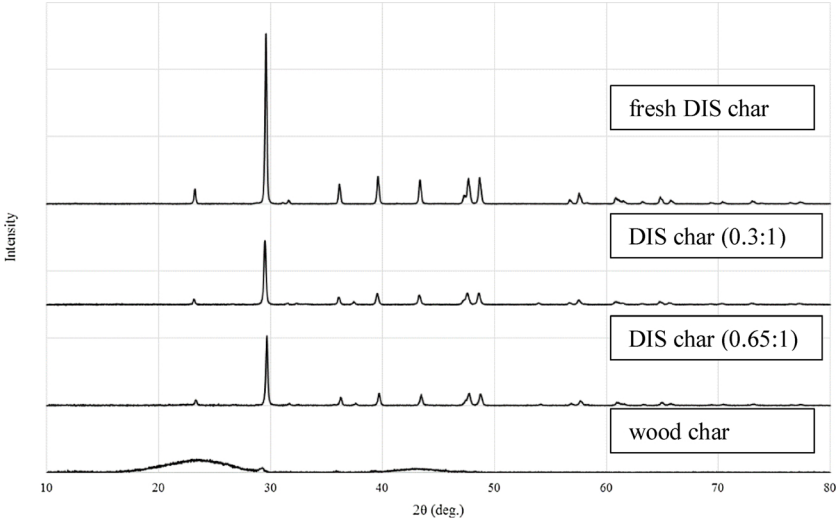

Fig. 9. X-ray diffraction pattern of DIS and wood char samples.

Acknowledgements

The authors would like to acknowledge the Engineering and Physical Sciences Research Council (EPSRC), Impact Acceleration Accounts (IAAs) and University of Birmingham for the financial support.

References

[1] A. Oasmaa, S. Czernik, Energy Fuels 13 (1999) 914.
[2] J. Lehto, A. Oasmaa, Y. Solantausta, M. Kytö, D. Chiaramonti, Appl. Energy 116 (2014) 178.
[3] A.V. Bridgwater, Biomass Bioenergy 38 (2012) 68.
[4] A. Fivga, L.G. Speranza, C.M. Branco, M. Ouadi, A. Hornung, AIMS Energy 7 (2019) 46.
[5] P. Bajpai, P. Bajpai Management of Pulp and Paper Mill Waste, Springer International Publishing, Cham, 2015 p. 9.
[6] Confederation of Paper Industries [CPI], Paper Myths and Facts: A Balanced View. CPI, Swindon, UK, (2012).
[7] R. Lou, S. Wu, G. Lv, Q. Yang, Appl. Energy 90 (2012) 46.
[8] M. Ouadi, J.G. Brammer, Y. Yang, A. Hornung, M. Kay, J. Anal. Appl. Pyrolysis 102 (2013) 24.
[9] A. Méndez, J.M. Fidalgo, F. Guerrero, G. Gascó, J. Anal. Appl. Pyrolysis 86 (2009) 66.
[10] N. Jäger, R. Conti, J. Neumann, A. Apfelbacher, R. Daschner, S. Binder, A. Hornung, Energy Fuels 30 (2016) 7923.
[11] L. Zhou, Z. Yang, A. Tang, H. Huang, D. Wei, E. Yu, W. Lu, J. Energy Inst. (2019).
[12] L. Zhang, B. Zhang, Z. Yang, Y. Yan, RSC Adv. 4 (2014) 39145.
[13] S. Vichaphund, V. Sricharoenchaikul, D. Atong, J. Anal. Appl. Pyrolysis 124 (2017) 568.
[14] A. Veses, M. Aznar, I. Martínez, J.D. Martínez, J.M. López, M.V. Navarro, M.S. Callén, R. Murillo, T. García, Bioresour. Technol. 162 (2014) 250.
[15] A. Veses, M. Aznar, M.S. Callén, R. Murillo, T. García, Fuel 181 (2016) 430.
[16] X. Chen, S. Li, Z. Liu, Y. Chen, H. Yang, X. Wang, Q. Che, W. Chen, H. Chen, Bioresour. Technol. 287 (2019) 121493.
[17] S.W. Banks, D.J. Nowakowski, A.V. Bridgwater, Energy Fuels 30 (2016) 8009.
[18] R. Mukhopadhyay, D. Kunzru, Ind. Eng. Chem. Res. 32 (1993) 1914.
[19] M. Ouadi, J. Brammer, M. Kay, A. Hornung, Appl. Energy 103 (2013) 692.
[20] Y. Shen, Y. Fu, Sustain. Energy Fuels 2 (2018) 326.
[21] Standard Test Method for Compositional Analysis by Thermogravimetry ASTM International E1131-03, (2003).
[22] J.P.A. Neeft, H.A.M. Knoef, G.J. Buffinga, U. Zielke, K. Sjöström, C. Brage, P. Hasler, P.A. Smell, M. Suomalainen, M.A. Dorrington, C. Greil, A.V. Bridgwater (Ed.), Progress in Thermochemical Biomass Conversion, 2008.
[23] W.L. Van de Kamp, P.J. De Wild, J.H.A. Kiel, U. Zielke, M. Suomalainen, H. Knoef, J. Good, T. Liliedahl, C. Unger, M. Whitehouse, J. Neeft, H. Van de Hoek, Energy Res. Cent. Neth. (ECN) (2005).
[24] C.E. Greenhalf, D.J. Nowakowski, A.V. Bridgwater, J. Titiloye, N. Yates, A. Riche, I. Shield, Ind. Crops Prod. 36 (2012) 449.
[25] J. Neumann, S. Binder, A. Apfelbacher, J.R. Gasson, P. Ramírez García, A. Hornung, J. Anal. Appl. Pyrolysis 113 (2015) 137.
[26] S. Hu, L. Jiang, Y. Wang, S. Su, L. Sun, B. Xu, L. He, J. Xiang, Bioresour. Technol. 192 (2015) 23.
[27] P. Gilbert, C. Ryu, V. Sharifi, J. Swithenbank, Bioresour. Technol. 100 (2009) 6045.
[28] D.J. Nowakowski, J.M. Jones, J. Anal. Appl. Pyrolysis 83 (2008) 12.
[29] F. Guo, X. Li, Y. Liu, K. Peng, C. Guo, Z. Rao, Energy Convers. Manage. 167 (2018) 81.
[30] N. Wang, D. Chen, U. Arena, P. He, Appl. Energy 191 (2017) 111.
[31] N. Gómez, S.W. Banks, D.J. Nowakowski, J.G. Rosas, J. Cara, M.E. Sánchez, A.V. Bridgwater, Fuel Process. Technol. 172 (2018) 97.
[32] J. Han, H. Kim, Renew. Sustain. Energy Rev. 12 (2008) 397.
[33] T. Hanaoka, T. Yoshida, S. Fujimoto, K. Kamei, M. Harada, Y. Suzuki, H. Hatano, S.-y. Yokoyama, T. Minowa, Biomass Bioenergy 28 (2005) 63.
[34] N. Tröger, D. Richter, R. Stahl, J. Anal. Appl. Pyrolysis 100 (2013) 158.
[35] X. Zhang, L. Sun, L. Chen, X. Xie, B. Zhao, H. Si, G. Meng, J. Anal. Appl. Pyrolysis 108 (2014) 35.
[36] X. Chen, Y. Chen, H. Yang, W. Chen, X. Wang, H. Chen, Bioresour. Technol. 233 (2017) 15.
[37] L. Ingram, D. Mohan, M. Bricka, P. Steele, D. Strobel, D. Crocker, B. Mitchell, J. Mohammad, K. Cantrell, C.U. Pittman, Energy Fuels 22 (2008) 614.
[38] R. Kumar, V. Strezov, T. Kan, H. Weldekidan, J. He, Energy Procedia 160 (2019) 186.
[39] Y. Elkasabi, C.A. Mullen, A.L.M.T. Pighinelli, A.A. Boateng, Fuel Process. Technol. 123 (2014) 11.
[40] A.V. Bridgwater, D. Meier, D. Radlein, Org. Geochem. 30 (1999) 1479.
[41] A. Arregi, M. Amutio, G. Lopez, M. Artetxe, J. Alvarez, J. Bilbao, M. Olazar, Energy Convers. Manage. 136 (2017) 192.
[42] R.J.M. Westerhof, D.W.F. Brilman, M. Garcia-Perez, Z. Wang, S.R.G. Oudenhoven, S.R.A. Kersten, Energy Fuels 26 (2012) 7263.
[43] Q. Lu, W.-Z. Li, X.-F. Zhu, Energy Convers. Manage. 50 (2009) 1376.
[44] J.E. Amonette, S. Joseph, Biochar for Environmental Management, Routledge, 2012, p. 65.
[45] S. Ren, H. Lei, L. Wang, Q. Bu, S. Chen, J. Wu, RSC Adv. 4 (2014) 10731.
[46] T.R. Carlson, J. Jae, Y.-C. Lin, G.A. Tompsett, G.W. Huber, J. Catal. 270 (2010) 110.
[47] Y. Zheng, L. Tao, Y. Huang, C. Liu, Z. Wang, Z. Zheng, J. Anal. Appl. Pyrolysis 140 (2019) 355.
[48] D. Wang, R. Xiao, H. Zhang, G. He, J. Anal. Appl. Pyrolysis 89 (2010) 171.
[49] Y. Baimark, N. Niamsa, Biomass Bioenergy 33 (2009) 994.
[50] Z. Rui, D. Wei, Y. Zhibin, Z. Chao, A. Xiaojuan, J. Chem. Pharm. Res. 6 (2014) 1254.
[51] A. Elloumi, M. Makhlouf, A. Elleuchi, C. Bradai, Polym. Technol. Eng. 55 (2016) 1012.
[52] X. Song, Y. Zhang, C. Chang, Ind. Eng. Chem. Res. 51 (2012) 15075.